The Villalbeto de la Peña Meteorite: Raman Spectroscopy and Cathodoluminescence of Feldspar

Garcia-Guinea[a], J., L. Sanchez-Muñoz[b], J. L. Tormo[a], E. Crespo-Feo[a], J. Ruiz-Perez[c], A.I. Martin-Herrero[d], A. Cremades[e]

[a]Museo Nacional Ciencias Naturales, Jose Gutierrez Abascal 2, Madrid 28006, Spain,;
[b]CIEMAT. Av. Complutense 22, Madrid 28040, Spain,
[c]Centro de Biología Molecular, CSIC-Universidad Autónoma de Madrid, 28049 Cantoblanco, Madrid, Spain. [d]Seminario de Ciencias Planetarias, Universidad Complutense de Madrid, 28040 Madrid, Spain.
[e]Dpto Fisica Materiales, Facultad de Fisicas, Universidad Complutense de Madrid, 28040, Spain.

Abstract. This paper mainly focuses on the spatial distribution of plagioclase phases observed by Raman and spectra cathodoluminescence (CL) emission of in the Villalbeto de la Peña meteorite. Initially, we collected fragments countryside to determine the strewn field area and to perform spot chemical analyses by electron microprobe for the classification of the specimens (L6 Chondrite). Furthermore, the hyperspectral Raman mapping allow us identify amorphous Maskelynite feldspar in plagioclase micro-fissures since it is a molecular technique. The spectra CL emission bands observed at circa 290, 340, 390, 440, 510, 640 and 780 nm are characteristic in aluminosilicate lattices providing additional data on H^+, OH^- and H_2O and Na^+ self-diffusion along interfaces (290 nm), on strained Si—O bonds (340 and 650 nm), on $[AlO_4]^\bullet$ centers (380-390 nm and 420-440 nm), on O^-—Si...M^+ centers (510 nm) and on substitutional Fe^{3+} in aluminum positions (740—800 nm broad band). The CL and hyperspectral Raman techniques coupling demonstrates that the Villalbeto meteorite was shock-metamorphosed from the amorphous Maskelynite presence in Plagioclase fissures and from the strained Si—O bonds at room temperature.

Keywords: Spectra-Cathodoluminescence, Hyperspectral-Raman, Maskelynite, Villalbeto-Meteorite, Plagioclase, Feldspars, Luminescence.

INTRODUCTION

The fall of the Villalbeto de la Peña [illegible] the best documented in history for which atmospheric and orbital trajectory, strewn field area, and recovery circumstances have been described in detail [1-2] (Fig. 1). Additional details on the bulk chemistry [3] and the bulk luminescence [4] were later provided. Moreover, the intrinsic complexity of composition, distribution and structural states of plagioclase crystals in L6 chondrite meteorites [5], such as the Villalbeto feldspars case, suggested us to perform this study by Electron Probe Microanalyses (EPMA), spatially-resolved spectra Cathodoluminescence (CL) and Hyperspectral-Raman contour-plot micro-analyses (Raman), exploring the Maskelynite-Plagioclase distribution of the studied fragments and the possible between relationships the CL emission bands and the common structural plagioclase features. The UV-blue region of the feldspar spectrum displays numerous broad bands, which are generally discussed in terms of intrinsic defects. In the case of intrinsic defects particularly, precise models are probably unfeasible because of the variety of lattice site distortions which arise in such a complex and variable mineral system. In despite of this difficulty, we try to manage possible defect-emission linkages on the basis of previous references and the most common plagioclase defects.

FIGURE 1. (a) First author (Garcia-Guinea) finding a fragment, (b) Detail of the meteorite in its original position, (c) Strewn field area outlined on the basis of 32 collected fragments together with their GPS positions.

EXPERIMENTAL

We study in polished sections of the L6-chondrite specimens collected by ourselves in Villalbeto and stored as international type reference samples in our National Museum of Natural Science of Madrid which also keeps circa the 95% of all the Spanish meteorite fragments. The Electron Probe Microanalyses (EPMA) analyses were performed by a Jeol Superprobe JXA-8900M and by Environmental Scanning Electron Microscopy with X-ray Dispersive Spectrometry probe (ESEM-EDS) in an Inspect-S ESEM of the FEI company. The hyperspectral Raman contour plots were performed using a new ThermoFischer Raman Microscope with one micron spatial resolution and a laser source at 532 nm. The hot CL spectra of plaglioclase grains were obtained by SEM-CL in a Hitachi S2500 electron microscope. Light emissions were focused with lens attached to the microscope window, and a light guide was used to feed the light into the CCD camera and the CL images were recorded using a Hamanatsu R-928 photomultiplier. The CL spectra were recorded with a Hamamatsu PMA-11 CCD cam-era. Cold CL images of Villalbeto feldspars distribution were taken in a optical CL 8200 MK4 system made by Cambridge Image Technology Ltd, with an electron beam exciting at 16 kV and a current of 0.5 mA/s.

RESULTS AND DISCUSSION

From the intensity of blue CL and BSE contrast in SEM images (Fig. 3), two different regions of feldspar composition have been observed: i) Maskelenite and Na-rich feldspars forming mixtures at a level lower than the resolution of optical microscopy techniques forming like-veins between other crystals and intergrowths with pyroxene; ii) extended volumes with homogeneous Na-rich feldspar crystalline structure. The results of the EPMA 45 spot analysis on feldspar phases are shown in both, Table 1, as some representative analyses of feldspar, and Figure 2, which displays the ternary Na2O—K2O—CaO compositions of Villalbeto feldspar samples. The Na-rich feldspars were also analyzed by transmission electron diffraction (TEM) and selected area electron diffraction (SAED) along [001] zone axis, in a microscope with an EDAX facility to correlate chemical, structural and micro-structural data. No twinning were identified in TEM images, diffraction spots do not show splitting, and a regular circular shape allow us to measure the γ^* angle being lower than 90^o, indicating a high or intermediate albite local ordering scheme in the Si/Al distribution.

TABLE 1. Spot Electron Probe Microanalyses of the most representative phases taken on feldspar zones of the Villalbeto L6 Chondrite.

	Bytownite	**Albite**	**Oligoclase**	**Maskelenite**	**Maskelenite**
SiO_2	64.63	64.87	66.15	67.84	68.81
Al_2O_3	17.58	21.18	22.87	23.28	22.96
FeO	1.41	0.44	0.54	0.31	0.66
MnO	0.01	0.00	0.08	0.00	0.00
MgO	3.76	0.01	0.02	0.00	0.03
CaO	8.20	2.36	2.51	2.24	2.16
Na_2O	2.75	9.91	6.87	3.99	2.67
K_2O	1.14	0.27	0.66	1.82	1.71
TiO_2	0.10	0.00	0.02	0.01	0.09
NiO	0.03	0.01	0.00	0.00	0.10
Cr_2O_3	0.15	0.00	0.00	0.00	0.02
P_2O_5	0.03	0.02	0.03	0.00	0.00
Total	99.79	99.07	99.75	99.49	99.21

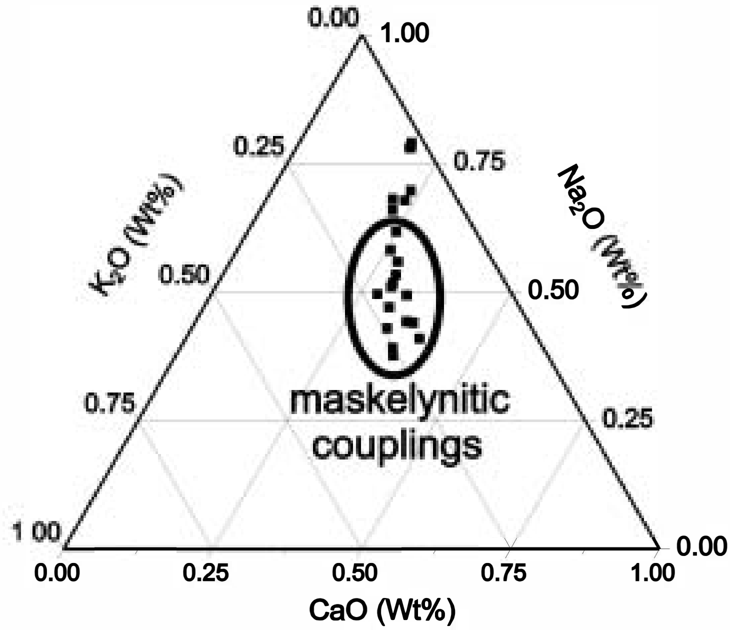

FIGURE 2. (a) Ternary alkalis plot (K2O—Na2O—CaO) of the spot EMPA analyses depicting maskelenitic compositions since this region is commonly empty in terrestrial feldspar.

Maskelenite was easily identified by the lack of structure in the electron diffraction spectra. We infer that our experimental results on metastable proportional K-Ca-Na compositions, sited in the triangle center, could be partially amorphous Maskelenite, together with crystalline plagioclase species, e.g., bytownite, albite, oligoclase (Table 1). The meteorite luminescence is mainly produced by feldspars, Figure 3a shows the cold CL plot distribution, as follows: (i) red spots, Bytownite with Mn^{2+} point defects in structural Ca positions, (ii) blue masses, Oligoclase with $[AlO_4]^o$ defects, (iii) Maskelenite sodium glasses with low UV-blue emission. Figure 2b&c displays the spatially-resolved hot CL spectra taken on the main feldspar masses observed under SEM in good agreement with the cold CL picture. A Hyperspectral Raman plot was also performed to explore the plagioclase crystal (Fig.3c and d). The maskelynite amorphous phase was mainly observed in the plagioclase fissures previously analysed in the ESEM microscope. The maskelynite Raman spectrum includes common peaks with plagioclases phases. Finally, Figure 3e depicts representative spectra CL taken from different regions on the feldspar areas. Fig 3f displays a representative spectrum CL of plagioclase with resolved peak maxima at 295, 331, 393, 442, 514, 653 and 774 nm.

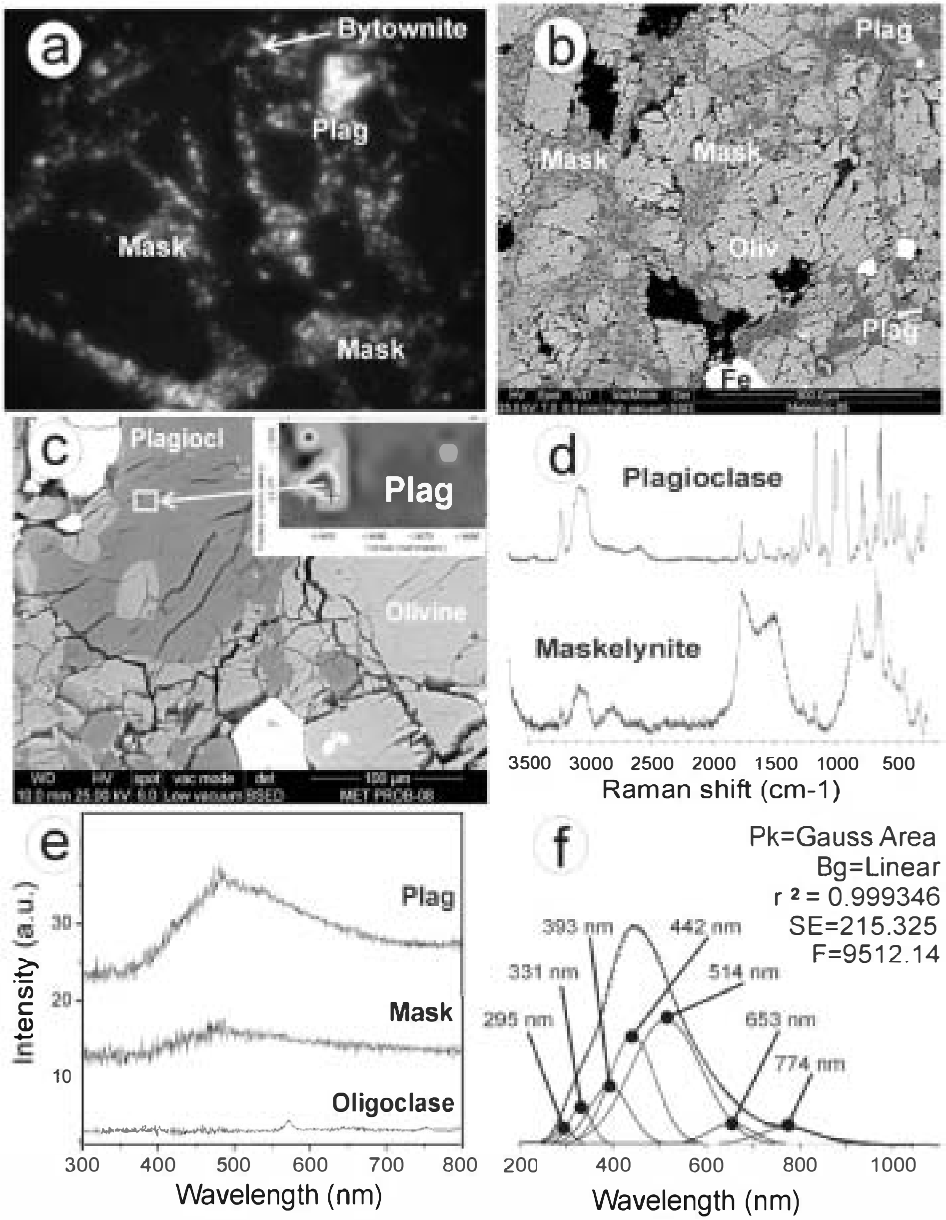

FIGURE 3. Villalbeto meteorite plagioclase feldspars: (a) Image of Cold CL by polarizing microscopy. (b) Backscaterring SEM image showing the feldspars spatial distribution, (c) Detail of maskelenite in fissures under SEM and region explored by an hyperspectral Raman plot contour, (d) Two representative Raman spectra of the plagioclasic phases, (e) CL spectra of some different plagioclase grains, (f) Deconvolution of a plagioclase CL spectrum exhibiting the classic spectra bands of plagioclase feldspars.

According to the defect-emission linkages for feldspars reviewed by Krbetschek et al. [6], we suggest that Villalbeto plagioclase display the general position bands in feldspars at 290, 340, 390, 440, 510, 640 and 780 nm (Fig. 3f). (i) The 290 nm CL emission is a irreversible thermolabile band of sodium plagioclase [7], which disappears with soft pre-heating, it has been also linked with metals Pb and Tl in amazonite fissures [8], all is true, since we test larger CL 290 nm emission in these hydrous zones of amazonite with metals, furthermore, it seems a better decisive factor to explain widespread emissions by collective feldspar features and not just only by scarce natural activators or rare elements; in the 290 nm case, common factors may be H^+, OH^- and H_2O and Na^+ self-diffusion along interfaces. (ii) the 340 nm emission CL is only observed at room temperature in stressed silicate lattices, such as the cases of hatch-crossed microclines, or in near all silicates recording ionoluminescence at low temperature [9]. (iii) the 380-390 nm and 420-440 were described in quartz [10] where prolonged high-temperature annealing of the samples in vacuum (10 h at 1400°C, 1 Pa) reduces the presence of ionic charge compensators at the Al sites and induces an intense 380 nm thermostimulated-luminescence (TSL) emission to $[AlO_4]^{\circ}$ centers. Prolonged strong annealing of aluminosilicate lattices (quartz, feldspars, feldspathoids, zeolites, etc.) remove alkali ions and produce intense blue TSL emissions (around 430 nm), these centers were also previously Al—O^- Al [11]. Plagioclase lattices may be sensitized, by thermal leakage of alkali ions, from very low temperature-time doses, (e.g. 80 °C for a few minutes to above 1400 °C for several months). These processes involve Na^+, K^+, OH), H^+ and H_2O exchanges with the environment. (iv) the 510 emission CL band was associated with O^-—Si…M^+ centers [12] being very common in framework silicates, (v) the red emission band at circa 650 nm is most intense in volcanic quartz specimens being associated with strained silicon-oxygen bonds [12] a similar stress could be found in strained meteorite plagioclase lattices such the Villalbeto case. Luminescence studies of feldspars have linked some impurity sites to specific emission bands, e.g. Fe with 720 nm or Mn to 560 nm emissions [13-15]. In Villalbeto plagioclase case, both emissions CL bands at 340 & 650 nm points to strained Si—O bonds, i.e., a possible tectonic origin for the fragments in accordance with other previous data reported indicating that Villalbeto meteorite was shock-metamorphosed [3].

REFERENCES

1. L. Llorca et al., *Meteoritics & Planet. Sci.*, **40**, 795—804 (2005).
2. J.M. Trigo-Rodriguez et al., *Meteoritics & Planet. Sci.,* **41**, 505—517 (2006).
3. J. Llorca et al., *Meteoritics & Planet. Sci.,* **41**, A177—A182 (2007).
4. V. Correcher V. et al., *NIM Phys Res. A*. **580**, 637—640 (2007).
5. Y. Nakamuta, and Y. Motomura, *Meteoritics & Planet. Sci.,* **34**, 763—772 (1999).
6. M.R. Krbetschek, J. Götze, A. Dietrich, T. Trautmann, *Radiat. Meas.* **27**,(5-6), 695—748 (1997).
7. J. Garcia-Guinea, J. Garcia-Guinea J, H.M. Rendell, L. Sanchez-Munoz, *Radiat Protec Dosim* **66**, 39—398 (1996).
8. B.S. Gorobets, M.L. Gaft, A.M. Podolsky, Luminescence of Minerals and Ores. Ministry of Geology. Moscow. USSR (1989).

9. J. Garcia-Guinea, V. Correcher, L. Sanchez-Munoz, A.A. Finch, D.E. Hole, P.D. Townsend, *NIM & Meth. Phys. Res. Section A* **580**, 648—651 (2007).
10. M. Martini, A. Paleari, G. Spinolo, A. Vedda, *Phys Rev B Cond Matter* **52**(1), 138—142 (1995).
11. A.S. Marfunin, Spectroscopy, Luminescence and Radiation Centers in Minerals. Springer. Berlin (1979).
12. A.S. Marfunin, and L.V. Bershov, *Dokl. Akad. Nauk*. **193**, 412-–414 (1970).
13. J. E. Geake, G. Walker, D. J. Telfer, A.A. Mills, *Phil. Trans. R. Soc. London A* **285**, 403-–408 (1977).
14. D.J. Telfer and G. Walker, *Mod. Geology* **6**, 199-210 (1978).
15. A. A. Finch, D.E. Hole, P. D. Townsend P. D., *Phys. Chem. Mineral*. **30**, 373—381 (2003).